

Effect of a Nonionic Surfactant on the Pseudoternary Phase Diagram and Stability of Microemulsion

by Aning Ayucitra

Submission date: 16-Jan-2024 04:37PM (UTC+0700)

Submission ID: 2271809304

File name: B1.22_JCED-0c00341_2020_Effect_of_nonionic_surfactant.pdf (2.21M)

Word count: 6843

Character count: 34411

Effect of a Nonionic Surfactant on the Pseudoternary Phase Diagram and Stability of Microemulsion

Chintya Gunarto, Yi-Hsu Ju, Jindrayani Nyoo Putro, Phuong Lan Tran-Nguyen, Felycia Edi Soetaredjo, Shella Permatasari Santoso, Aning Ayucitra, Artik Elisa Angkawijaya,* and Suryadi Ismadji*

Cite This: *J. Chem. Eng. Data* 2020, 65, 4024–4033

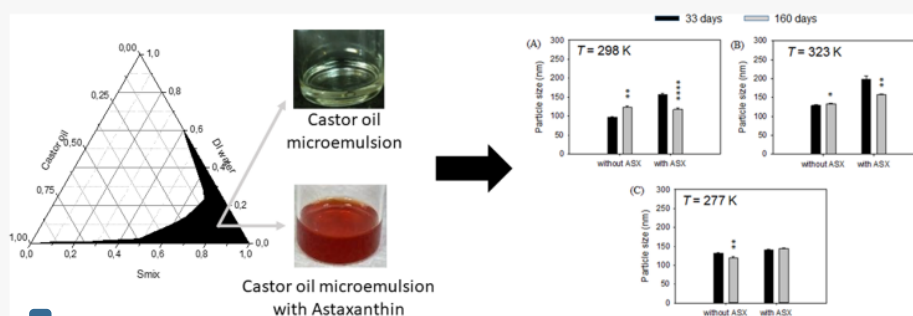
Read Online

ACCESS |

Metrics & More

Article Recommendations

Supporting Information



ABSTRACT: Microemulsion (ME) is a micron-sized droplet that consists of oil and water, with addition of a surfactant and cosurfactant. Recently, ME is widely used in biomedical application for proper drug delivery in the human body. Castor oil as the oil phase, Tween 80 or Tween 20 as the surfactant, glycerol or ethanol as the cosurfactant, and DI water as the water phase were used for ME preparation in this study. The effect of the surfactant-to-cosurfactant ratio on the pseudoternary phase diagram was investigated. The as-synthesized ME with the composition of 5 wt.% castor oil, 85 wt.% surfactant mixture, and 10 wt.% water was characterized based on its particle size, polydispersity index, and zeta potential. From that composition, the largest ME was attained at an S_{mix} 2 weight ratio of tween 80 to ethanol. Astaxanthin as lipophilic drug substance was used as the model drug for the ME encapsulation study. The thermal and storage analysis test of ME and astaxanthin-loaded ME demonstrated the stability of the as-synthesized ME and its analogous drug-loaded form.

1. INTRODUCTION

Astaxanthin (ASX, $C_{40}H_{52}O_4$, Figure 1) is one of the most potent antioxidants, ubiquitously found in red-pigmented plants, bacteria, marine animals such as shrimp, salmon, and crab, flamingos, and microalgae.^{1,2} ASX is classified as a polar xanthophyll that functions as the cells' and tissues' protectant from the damaging effect of free radicals and single oxygen, thus it is able to inhibit cancers and tumors.³ In addition, it also could be used to prevent hypertension and cardiovascular diseases, as a stabilizer for beverages, and as anti-inflammatory substance.^{4–6} Despite its various health benefits, oral administration of ASX is impractical due to its eminent lipophilic nature.⁷ Thus, it is necessary to combine ASX with lipid for its optimal absorption and functionalization.⁸

Microemulsion (ME) is a lipid-based formulation that combines two immiscible liquids to form thermodynamically stable droplets with sizes between 100 and 300 nm. The basis in forming ME is to reduce interfacial free energy to a very low value, thus formation of ME is spontaneous.⁹ The application of ME may vary from the environmental sector by restoration

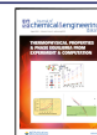
of oil spillage from a polluted area to pharmaceutical application where ME acts as drug carrier.¹⁰ Aside from promoting absorption of lipophilic drugs, adaptation of ME in medical usage reportedly may protect the drug against oxidation and enzymatic degradation.^{11,12}

Addition of a surfactant and/or cosurfactant in ME reportedly can decrease surface tension of the oil–water interface, stabilize the connection between lipophilic molecules and the aqueous phase, and enhance the solubility of hydrophobic drugs.^{13,14} Thus, selection of the surfactant and cosurfactant is crucial for proper ME formation. The hydrophile–lipophile balance (HLB) of different types of surfactants is listed in Table 1. A study by Shama indicated

Received: April 16, 2020

Accepted: July 22, 2020

Published: August 3, 2020



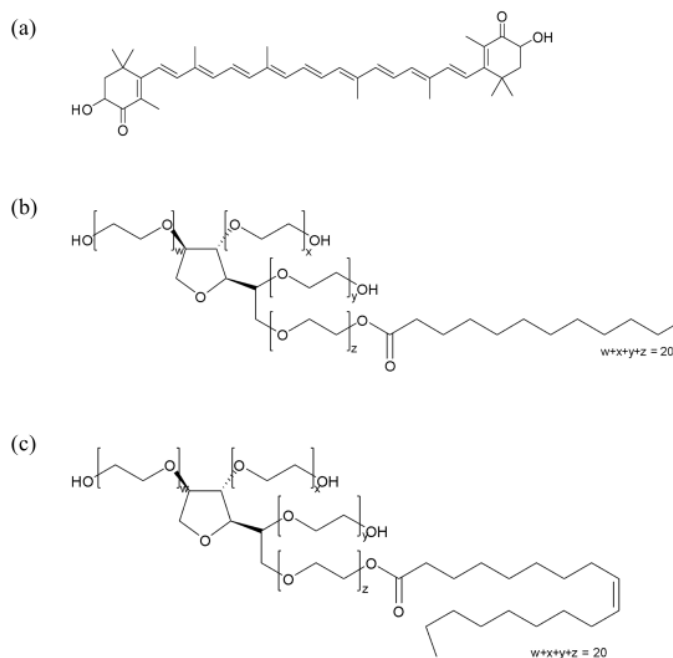


Figure 1. Molecular structure of (a) astaxanthin, (b) Tween 20, and (c) Tween 80.

Table 1. HLB Value of Different Surfactants

type	surfactants	HLB	ref
anionic	sodium dodecyl sulfate	40	43
	sodium stearyl-2-lactylate	2–3	16
cationic	didecyltrimethylammonium chloride	n.d. ^a	44
	cetyltrimethylammonium bromide	10	45
nonionic	T80	15.9	17
	T20	16.7	17
	Triton X	13.4	18

^an.d. = Not determined.

that the HLB value of 8–18 could synthesize oil in water ME, while those ranging from 3 to 6 resulted in water in oil ME.¹⁵ As a model drug, ASX is lipophilic, which required an oil-in-water ME system for the encapsulation. As listed in Table 1, several surfactants such as cetyltrimethylammonium bromide, T80, T20, and Triton X have an HLB value within this range. Toxicity of the surfactant was taken into account for the drug delivery purpose. Reportedly, a nonionic surfactant has the least toxicity compared to cationic and anionic surfactants.¹⁶ The lethal dose (LD₅₀) of T80 is 22,000 mg/kg while for T20

is 5000 mg/kg and for Triton X is >1000 mg/kg in rat (oral).^{17,18} Therefore, T80 and T20 were selected in this study.

For the later applications, oleic acid, salicylic acid, and vegetable oils from soybean, sunflower, peanut, castor, and olive were commonly used as the oil phase.^{19–21} Previous studies using nonionic surfactants demonstrated the superiority of ME as a carrier for lipophilic drugs, such as metformin hydrochloride, tamoxifen citrate, and probucol. These studies either used T20 or T80 as the surfactant, with a number of cosurfactants such as Cremophor EL, glycerin, Span 80, ethanol, and PEG-400. Encapsulation of these lipophilic drugs was postulated to decelerate the drug release and promote the drug absorption through an oral route.¹¹ As presented in Table 2, encapsulation of probucol into MEs improved the bioavailability up to 10.22 folds from the drug solution.²²

In this work, the effects of oil, surfactant, and cosurfactant composition on the formation, size, dispersibility, and stability of ME were studied. As the drug carrier matrix, the usage of harmless initial materials for ME formulation is necessary. Here, castor oil was used as the oil phase since it possesses anti-inflammatory properties owing to the presence of ricinoleic acid as its active fatty acid.²³ A study by Putro et al. reported the relatively harmless nature of the nonionic

Table 2. Microemulsion Formulated with Nonionic Surfactants for Drug Carrier Application

surfactant	cosurfactant	oil phase	drug	bioavailability in ME ^a	ref
T80	glycerin, Span 80	sesame oil	tamoxifen citrate	n.d. ^b	40
T20, Labrafil M 1944	Transcutol P	Capmul MCM C8	cilostazol	1.43	46
T80	PEG-400	olive oil	famotidine	n.d. ^b	11
T80, Cremophor EL	ethanol, Span 80	glyceryl monooleate, linoleic acid glyceride	metformin hydrochloride	1.14–1.47	47
T80, Cremophor EL	PEG-400	olive oil	probucol	2.15–10.22	22

^aFold change relative to drug without carrier. ^bn.d. = Not determined.

surfactant compared to anionic or cationic surfactants.²⁴ Thus, nonionic tween 20 or tween 80 (Figure 1) and ethanol or glycerol were used as the surfactant and cosurfactant, respectively, to enhance drug delivery by ME while maintaining the safeness of the system.²⁵ ASX was used as the model drug with the aim to investigate the stability of ME as a drug carrier matrix.

2. MATERIALS AND METHODS

2.1. Materials. Astaxanthin (purity >97%) and castor oil were purchased from Sigma-Aldrich (Lanhasire, UK). Surfactants polyoxyethylene (20) sorbitan monooleate (Tween 80, T80) and polyoxyethylene (20) sorbitan monolaurate (Tween 20, T20) were supplied by Wako Chemicals Industry (Osaka, Japan). Their molecular structures are shown in Figure 1. Ethanol (99.5%) obtained from Echo Chemical (Taiwan) and propane-1,2,3-triol (glycerol) purchased from JT Baker Chemicals (USA) were used as cosurfactants. The chemical details are listed in Table 3.

Table 3. Chemical Information

chemical name	chemical formula	CAS number
astaxanthin	C ₄₀ H ₅₂ O ₄	472-61-7
castor oil		8001-79-4
polyoxyethylene (20) sorbitan monooleate	C ₆₄ H ₁₂₄ O ₂₆	9005-65-6
polyoxyethylene (20) sorbitan monolaurate	C ₅₈ H ₁₁₄ O ₂₆	9005-64-5
ethanol	CH ₃ CH ₂ OH	64-17-5
glycerol	C ₃ H ₈ O ₃	56-81-5

2.2. Construction of the Phase Diagram. The construction of the pseudoternary phase diagram of ME followed the procedure of de Oliveira Neves and colleagues with slight modification.²⁶ The surfactant and cosurfactant were mixed with a fix weight ratio (S_{mix}) of 2:1, 1:1, and 1:2. Subsequently, mixtures of castor oil and S_{mix} were prepared at weight ratios of 10:1, 8:1, 6:1, 3:1, 2:1, 1:1, 1:2, 1:3, 1:6, 1:10, and 1:50 to cover all region in the phase diagram. To obtain a pseudoternary phase diagram of the ME, deionized (DI) water was added dropwise to castor oil and S_{mix} mixture and vortexed until homogeneous. From visual observation, the transparent and one-phase liquid is considered as an ME. By varying weight ratios, pseudoternary phase diagrams were plotted, and the ME area was calculated using Origin software. Calculation of the ME area in the pseudoternary graph was used to obtain the composition and the weight ratio of the components in the mixture. The area of ME was obtained from Origin, and eq 1 was used to obtain the percentage area in the pseudoternary phase diagram.

$$\%area = A/0.5 \times 100 \quad (1)$$

where A = ME area from Origin software, and 0.5 = ternary area.

2.3. Preparation of Astaxanthin-Loaded ME. The optimum weight ratio of the oil, surfactant, and cosurfactant that generates the largest-sized ME in the pseudoternary phase diagram was adopted for ASX-loaded ME (ME@ASX) preparation. Prior to ASX loading, a certain amount of ASX was solvated in castor oil to produce a 200 $\mu\text{g}/\text{mL}$ ME@ASX solution. Subsequently, this ASX–castor oil solution was mixed with 85 wt. % S_{mix} and DI water.

2.4. Characterization of ME and ME@ASX. The effects of various surfactants and cosurfactants on the stability of ME were investigated at three temperatures (277, 298, and 323 K) for 160 days. The stability of ME was examined based on its particle size, polydispersity index (PDI), and zeta potential by a zeta potential and particle size analyzer (ZetaPALS, Brookhaven Zeta Plus). The analyses were done at 298 K and a fixed angle of 90°. Zeta potential values were obtained using the Smoluchowski model. ME samples were diluted 50-fold with DI water for ZetaPALS measurement. Triplicate analyses were carried out for each condition. Phase stability of ME with the largest area was also observed by centrifugation at 3500 $\times\text{g}$ for 30 min, % transmittance (%T) measurement by a UV–vis spectrophotometer at 650 nm (UV-2600, Shimadzu, Japan), and viscosity determined by a Brookfield DVI viscometer.

2.5. Statistics Data Analysis. The data analysis was performed by one-way analysis of variance (ANOVA) and the Tukey test using Minitab 17. A p -value of <0.05 and different letters was considered statistically significant. The measurements were conducted in triplicate with a confidence interval (CI) range of 95%.

3. RESULTS AND DISCUSSION

3.1. Pseudoternary Phase Diagram. The phase diagram of castor oil, S_{mix} , and DI water with S_{mix} ratios of 2, 1, and 1/2 was calculated and constructed to obtain the ME region. MEs are classified into four Winsor types: Winsor type I, II, III, and IV. This study only focused on ME Winsor type IV, which is a one phase and transparent system.²⁷ As presented in Figure 2, the black-colored area in the pseudoternary phase diagram represents the clear, transparent, and one-phase region as ME, while the white-colored area represents turbid and white-colored solution. This turbid appearance can be observed when the weight ratio of oil/ S_{mix} was higher than 2, which suggests that the addition of the surfactant and cosurfactant is essential to suppress surface tension between oil and aqueous phases.

As presented in Figure 2a–c, with the increasing amount of ethanol in the system (S_{mix} 2, 1, and 1/2), the ME region of the T20 system decreased from 12.48 to 12.33%. Similarly, in the system containing the T80 surfactant (Figure 2d–f), the ME region was reduced from 16.92 to 16.54% with each ethanol addition. A similar trend was reported by Waisnoicharoen et al., where it was postulated that the addition of a cosurfactant may drag the system out of the ME region.²⁸ These results suggest that less ethanol as a cosurfactant may generate a broader ME region. However, excessive reduction of the cosurfactant in the system (S_{mix} ratio 4/1; pseudoternary phase diagram not shown) led to the reduction of the ME region (11.38 \pm 0.01% for T20 and 16.16 \pm 0.47% for T80, respectively). Thus, adequate addition of the cosurfactant is important for the formation of ME. $S_{mix} = 2$ (Figure 2a,d) gave the widest area of the ME region compared to the other studied ratios where T80-containing ME has a greater area (16.92 \pm 1.69%) compared to the one containing T20 (12.48 \pm 2.35%). The bigger area of the ME region in T80-containing ME might be attributed to the more hydrophobic nature of T80 (HLB 15.9) compared to T20 (HLB 16.7), thus favoring the solubilization of large molecular volume oil.^{29,30}

Besides ethanol, glycerol is another commonly used cosurfactant due to its cheap and nontoxic nature.³¹ Since the largest ME area for both T20 and T80 was obtained at S_{mix}

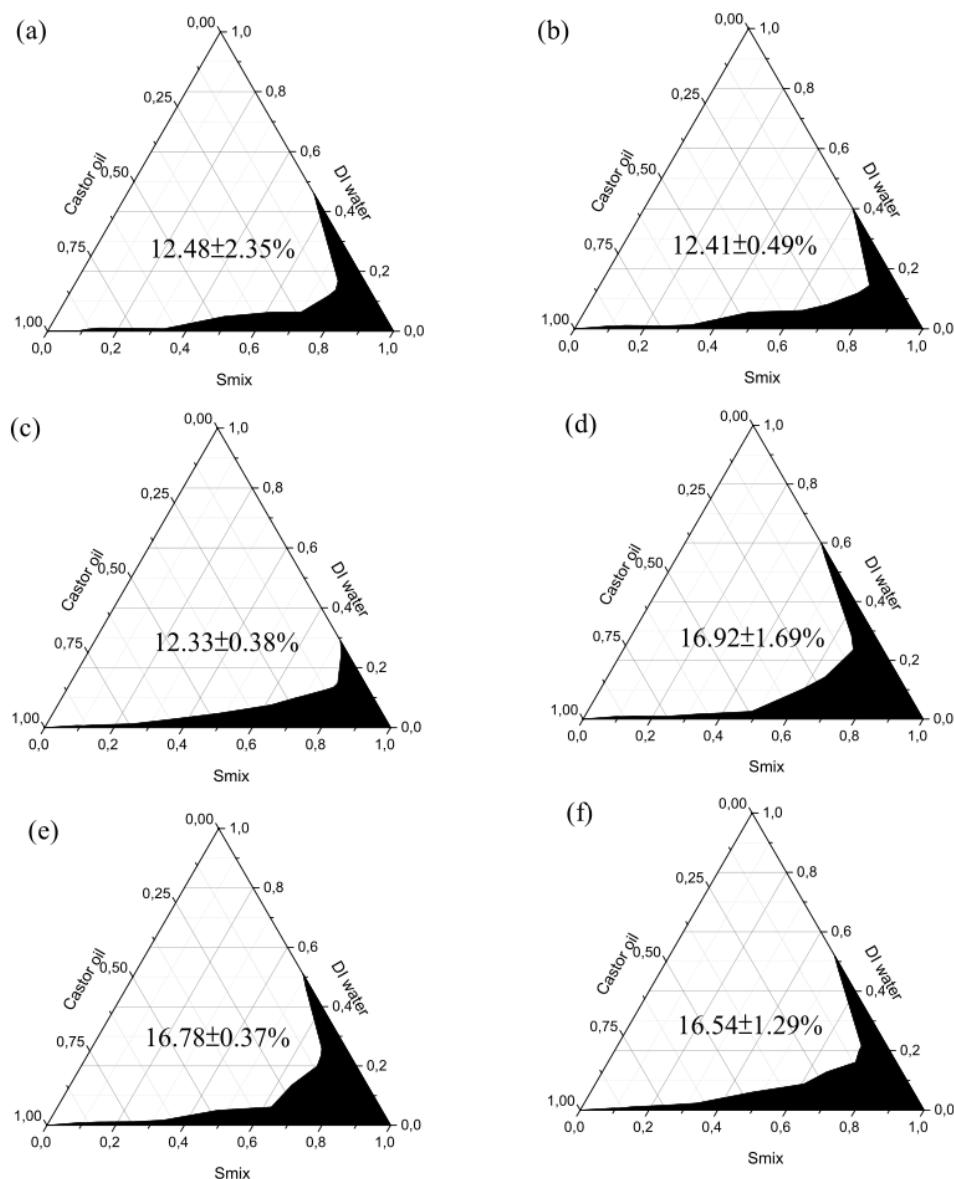


Figure 2. Pseudoternary graph of castor oil with T20 as the surfactant and ethanol as the cosurfactant at an S_{mix} of (a) 2, (b) 1, (c) 1/2; with T80 as the surfactant and ethanol as the cosurfactant at an S_{mix} of (d) 2, (e) 1, (f) 1/2. The black-colored area refers to the clear, transparent, and one-phase ME region.

= 2 (surfactant/cosurfactant ratio), substitution of ethanol by glycerol was carried out at the same ratio, and the pseudoternary phase diagrams obtained are presented in Figure 3. Addition of glycerol with nonionic surfactants resulted in a significant decrease in the ME area and the formation of a unique phase, known as the liquid crystal (LC, the gray area), which formed due to the repulsive interaction between the concentrated surfactant and glycerol. According to the study by Li et al., the LC phase could be recognized by increasing viscosity in the system.³² To confirm the formation of the LC in each system, a mixture composed of 10 wt.%

castor oil, 85 wt.% S_{mix} (T20/Gly), and 5 wt.% DI water was prepared, and its viscosity was measured. Compared to the one synthesized within the ME region (5 wt.% castor oil, 90 wt.% S_{mix} and 5 wt.% DI water), the viscosity of the LC is significantly higher (430.6 ± 3.39 cP for the LC and 302.15 ± 0.35 cP for the ME region). Similarly, the LC formulated with T80 (5 wt.% castor oil, 90 wt.% S_{mix} and 5 wt.% DI water) also showed higher viscosity (581.6 ± 4.8 cP) compared to the one in the ME region (551.95 ± 0.64 cP). Since ethanol is a short-chain alcohol, it may prevent the formation of any liquid crystal phase due to low interaction force.¹¹ The summary of

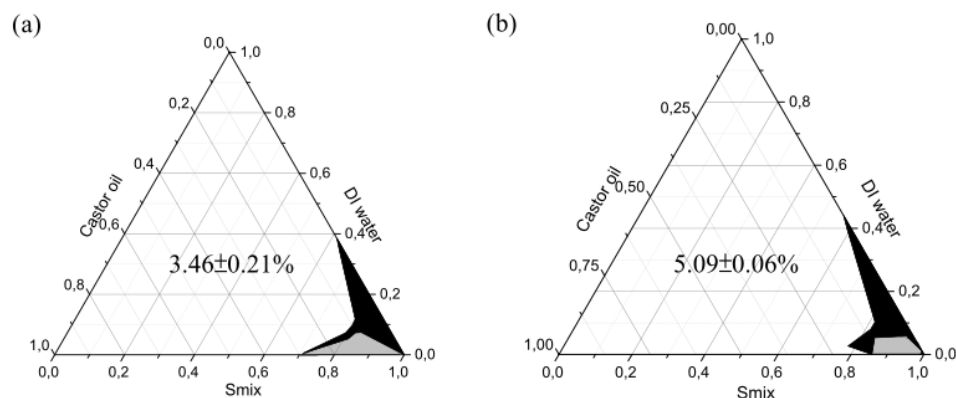


Figure 3. Pseudoternary phase diagram of (a) Tween 20 and (b) Tween 80 with glycerol as the cosurfactant at a weight ratio of 2. The black-colored area refers to the clear, transparent, and one-phase ME region. The grey-colored area refers to the liquid crystal region.

ME areas generated from different types and weight ratios of the surfactant and cosurfactant is listed in Tables 4 and 5. Overall, ethanol tends to produce a larger ME area for all S_{mix} ratios compared to the system containing glycerol as the cosurfactant.

Table 4. Selected Microemulsion Formulations (wt.%) and Characterization of T20 as a Surfactant from Figure 4a

parameter	1	2	3 ^a
castor oil	0.04	0.10	0.05
$S_{mix} = 2$	0.74	0.80	0.85
DI water	0.22	0.10	0.10
particle size (nm)	127.60 ± 24.92	163.57 ± 0.90	178.03 ± 9.72
PDI	0.48 ± 0.06	0.22 ± 0.22	0.23 ± 0.04

^aSelected formulation for further study.

Table 5. Selected Microemulsion Formulations (wt.%) and Characterization of T80 as a Surfactant from Figure 4b

parameter	1	2	3 ^a
castor oil	0.10	0.11	0.05
$S_{mix} = 2$	0.70	0.79	0.85
DI water	0.20	0.10	0.10
particle size (nm)	171.7 ± 4.47	108.78 ± 9.22	117.43 ± 0.38
PDI	0.25 ± 0.02	0.41 ± 0.11	0.31 ± 0.02

^aSelected formulation for further study.

To ensure that similar ME formulation can consistently be obtained while using a surfactant produced from different suppliers, a pseudoternary diagram of a system containing T20 from different brands (obtained from Acros, Belgium) is plotted in Figure S1. The system containing T20 from Acros produced 11.91 ± 0.39% area of the ME region (Figure S1), which is comparable to the one obtained using T20 from Wako (12.48 ± 2.35%). A study by Nazar et al. investigated the formulation of ME composed of castor oil/T80/ethanol/phosphate buffer, with T80 obtained from Fluka.³³ The ME region reported by Nazar et al. is comparable to the one obtained in this study. These results confirm the reliability of the generated pseudoternary diagrams.

Salinity of the aqueous solution and temperature of the system were postulated to have an effect on the solubilization

capacity of ME, which may later affect the pseudoternary phase diagram structure.^{34,35} The solubilization capacity of ME at a salt concentration of 0–0.35 M NaCl was measured according to Bera et al.³⁶ The highest solubilization of ME was achieved at a salt concentration of 0.14 M, which is desirable since it mimics the salt concentration in body fluid. To investigate the effect of the temperature on the pseudoternary phase diagram, a temperature of 310 K was used. This temperature was chosen to simulate the human body condition for later application. As presented in Figure S2, the area of ME constructed by the same mixture (castor oil, T80, EtOH, and DI water) at 310 K was slightly larger (18.49 ± 0.22%) than the one constructed at room temperature (16.92 ± 1.69%). This result is in agreement with Bera et al., which reported that a broader ME area can be achieved with an increasing temperature and salinity.³⁷

3.2. Characterization of ME. The larger ME area in the pseudoternary phase diagram may facilitate a wider range of alternate composition for ME synthesis. Several formulations of ME at different ratios of oil, S_{mix} , and water were selected (Figure 4) and characterized, and the results are shown in Tables 4 and 5. In all formulations, the formation of ME with a droplet size less than 200 nm and a PDI value less than 0.5 was confirmed. It can be observed that the PDI value of T20–ME formulation 1 (0.48) is close to the limit of the monodisperse system. The same phenomenon can be seen in T80–ME formulation 2 (PDI value = 0.41). Based on this result, ME with formulation 3, which consists of 5 wt.% castor oil, 85 wt.% S_{mix} , and 10 wt.% water was selected for further investigation. To confirm the presence of the surfactant and cosurfactant in the system, the HPLC chromatogram of ME with formulation 3 was plotted (Figure S3).

ME was characterized based on the particle size and dispersion homogeneity of its micelle. As listed in Table 6, in the T20E-1 system composed of T20 as the surfactant and ethanol as the cosurfactant at an S_{mix} ratio of 2 has a particle size of 178.03 ± 9.72 nm. The particle size in T20E-2 and T20E-3 systems, which consist of T20 and ethanol with S_{mix} ratios of 1 and 1/2, respectively, are 150.73 ± 2.64 and 213.13 ± 0.9 nm. Substitution of glycerol as the cosurfactant greatly affected the particle size of the ME to 280.57 ± 39.83 nm for the T20G system at an S_{mix} ratio of 2. For the T80-containing system, T80E-1, which consists of T80 (surfactant), ethanol

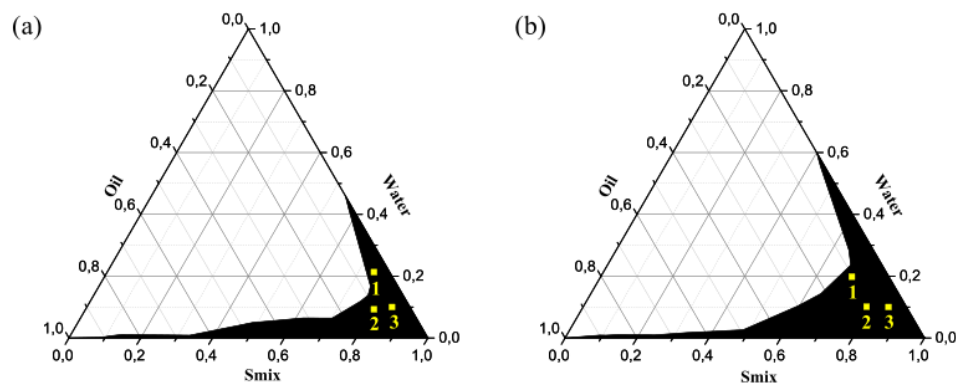


Figure 4. Pseudoternary phase diagram of (a) T20 or (b) T80 as the surfactant and ethanol as the cosurfactant with an S_{mix} of 2. Yellow numberings inside the diagrams were the selected compositions for initial characterization.

Table 6. Particle Size and the PDI for Selected Microemulsion at $T = 298$ K ($n = 3$, Mean \pm SD)

codes	cosurfactant	S_{mix}	ME Area (%)	ME at 5 wt.% castor oil, 85 wt.% S_{mix} , and 10 wt.% water	
				particle size (nm)	PDI
Tween 20					
T20E-1	ethanol	2	12.48 \pm 2.35	178.03 \pm 9.72	0.23 \pm 0.04
T20E-2	ethanol	1	12.41 \pm 0.49	150.73 \pm 2.64	0.20 \pm 0.04
T20E-3	ethanol	1/2	12.33 \pm 0.38	213.13 \pm 0.90	0.16 \pm 0.02
T20G	glycerol	2	3.46 \pm 0.21	280.57 \pm 39.83	0.15 \pm 0.07
Tween 80					
T80E-1	ethanol	2	16.92 \pm 1.69	117.43 \pm 0.38	0.31 \pm 0.02
T80E-2	ethanol	1	16.78 \pm 0.37	150.50 \pm 9.17	0.25 \pm 0.06
T80E-3	ethanol	1/2	16.54 \pm 1.29	139.17 \pm 2.25	0.25 \pm 0.01
T80G	glycerol	2	5.09 \pm 0.06	260.87 \pm 2.02	0.21 \pm 0.03

(cosurfactant) with an S_{mix} ratio of 2, has a particle size of 117.43 ± 0.38 nm. Similar to the T20-containing system, at the same S_{mix} , the use of glycerol as the cosurfactant produced bulkier ME (260.87 ± 2.02 nm). As shown in Table 6, all ME had an initial size of less than 300 nm, which can be classified as ME.³⁸

The homogeneity of the system was examined and expressed as a PDI value. For the T20-containing systems, namely, T20E-1, T20E-2, T20E-3, and T20G, the PDI values are 0.23 ± 0.04 , 0.20 ± 0.04 , 0.16 ± 0.02 , and 0.15 ± 0.07 , respectively. Similarly, in the T80-containing systems, the PDI value ranges from 0.21 to 0.31 as listed in Table 6. The PDI values of all prepared ME are less than 0.5, indicating homogeneous dispersion and long-term stability of ME.^{39,40} Besides the PDI, surface charge of ME is an important property related to particle repulsion in the system to inhibit agglomeration and prolong its stability.^{41,42} The surface charges of the MEs synthesized in various compositions were shown to be negative with magnitude ranging from -11.59 to -8.08 (Figure 5). The high zeta potential value might be attributed to hydrogen bonding between the hydroxyl group of ricinoleic acid in castor oil and the nonionic surfactant.

3.3. Astaxanthin-Loaded ME. Preparation of ME@ASX was similar to that of ME. Instead of castor oil only, ASX in castor oil solution was added to the system. The pseudoternary phase diagram of ME@ASX (data not shown) for $S_{mix} = 2$ with ethanol as the cosurfactant yielded an ME area of 11.54 ± 0.3 and $18.4 \pm 0.25\%$ for T20 and T80, respectively. Observation of ASX loading in the ME was conducted by particle size

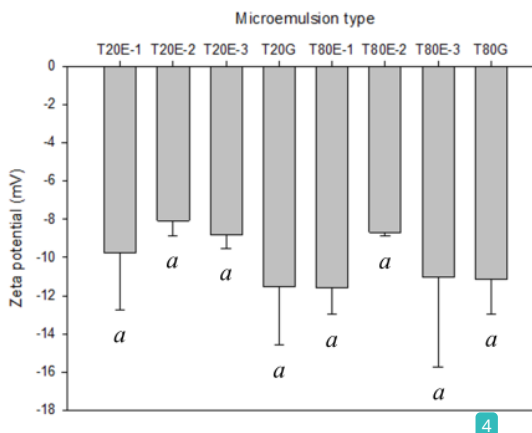


Figure 5. Zeta potential of freshly selected microemulsions. Different letters indicate significant differences among formulations. Multiple comparisons of means were performed using Tukey's test at the 0.05 significance level.

measurement. From Figure 6a, it can be seen that encapsulation of ASX resulted in bigger particle size for T20 or T80 as the surfactant and ethanol as the cosurfactant. Encapsulation of ASX enlarges the particle size of T20E-1 from 178.03 to 197 nm and T80E-1 from 117.43 to 198.8 nm. Additionally, the ME@ASX displayed an orange-red color,

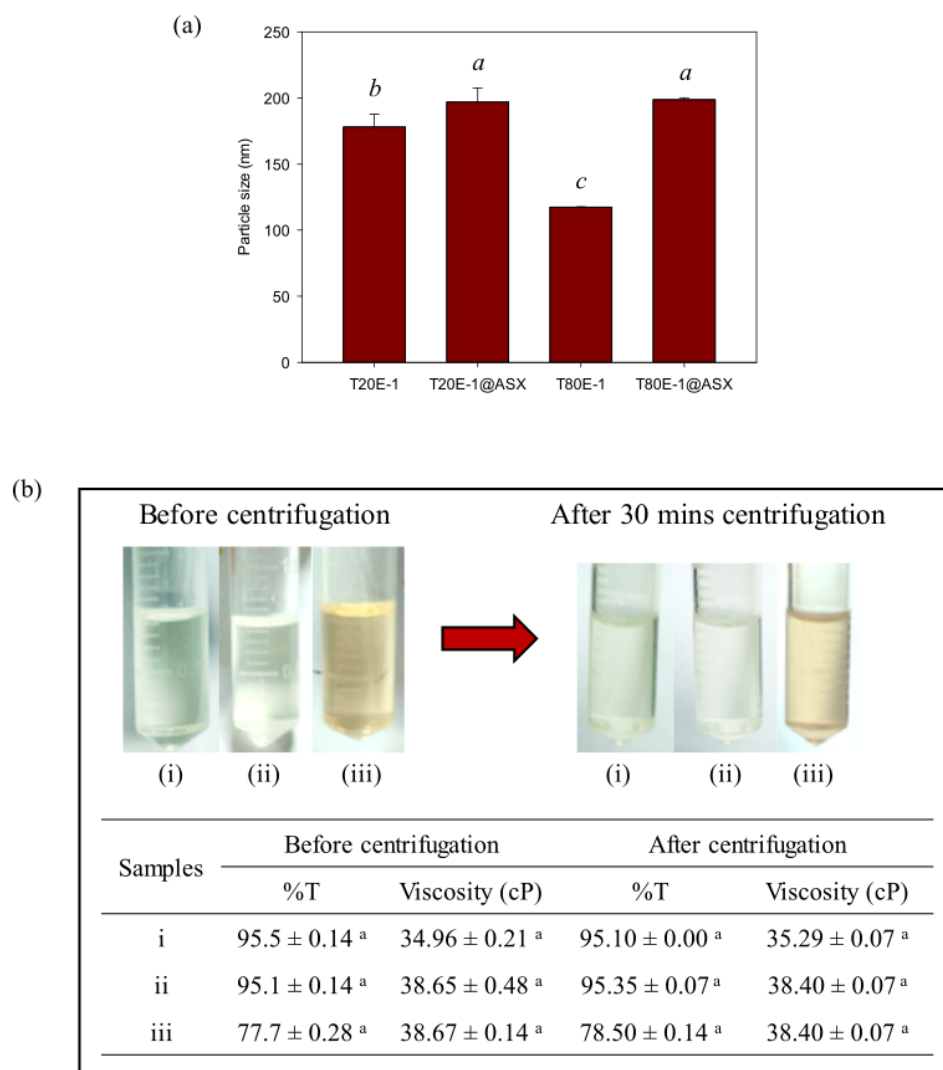


Figure 6. (a) Particle size comparison of microemulsion loaded with ASX (ME@ASX) and microemulsion without ASX. (b) Physical appearance and quantitative characterization before and after centrifugation of (i) T80E-1, (ii) T20E-1, and (iii) T80E-1@ASX. Different letters indicate significant differences among formulations. Multiple comparisons of means were performed using Tukey's test at the 0.05 significance level.

which demonstrated the successful encapsulation of red-colored ASX into ME (Figure 6b).

3.4. Stability Study of ME and ME@ASX. To investigate the effect of gravitation force on the ME system, MEs with and without ASX loading were centrifuged at 3500 \times g for 30 min, and the results are presented in Figure 6b. After undergoing centrifugation, the transparency and the viscosity of MEs were quantified. Both T20- and T80-containing MEs show high %T (> 95), which confirms the transparency of the systems. Compared to the one before centrifugation, no significant difference can be observed in the %T of T20E-1, T80E-1, and T80E-1@ASX. Determination of the ME viscosities before and after centrifugation further demonstrated the stability of T20E-1, T80E-1, and T80E-1@ASX. The viscosity of all tested systems ranges from 34.96 to 38.67 cP. Statistical significance

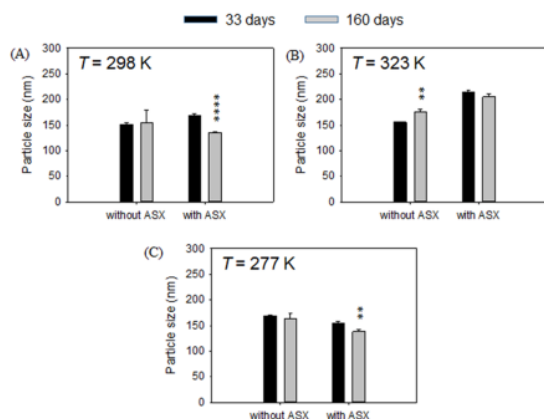
analysis confirms that there is no significant change in the %T and viscosity in all systems (including the one after ASX encapsulation). This suggests that the formulated ME was stable against the centrifugation process, thus centrifugation did not affect the properties of all formulated MEs and ME@ASX. No color change, precipitation, nor phase separation was observed after centrifugation.

Stability of ME was confirmed through a storage test. After 160 days of storage at 277, 298, and 323 K, the system remained homogeneous with the polydispersity index unchanged (0.2–0.3, Table 7). MEs with $S_{\text{mix}} = 2$ for T20 and T80 with ethanol were selected for ZetaPALS measurement due to the largest ME region in the pseudoternary phase diagram. After 160 days, the particle sizes of ME and ME@ASX at 298 K (T80E-1) were maintained at 122.63 and 177.43

Table 7. Polydispersity Index of Microemulsions with and without ASX at Different Temperatures for Storage up to 160 Days ($n = 3$, Mean \pm SD)

time storage (days)	samples	polydispersity index at T		
		298 K	323 K	277 K
0	T20E-1		0.23 \pm 0.04	
	T20E-1@ASX		0.24 \pm 0.05	
	T80E-1		0.31 \pm 0.02	
	T80E-1@ASX		0.25 \pm 0.01	
33	T20E-1	0.23 \pm 0.04	0.24 \pm 0.03	0.24 \pm 0.01
	T20E-1@ASX	0.28 \pm 0.02	0.29 \pm 0.03	0.27 \pm 0.01
	T80E-1	0.30 \pm 0.02	0.30 \pm 0.01	0.27 \pm 0.03
	T80E-1@ASX	0.22 \pm 0.01	0.24 \pm 0.04	0.30 \pm 0.02
160	T20E-1	0.20 \pm 0.12	0.24 \pm 0.01	0.20 \pm 0.05
	T20E-1@ASX	0.25 \pm 0.03	0.21 \pm 0.03	0.26 \pm 0.01
	T80E-1	0.28 \pm 0.01	0.26 \pm 0.04	0.28 \pm 0.03
	T80E-1@ASX	0.29 \pm 0.01	0.30 \pm 0.01	0.28 \pm 0.01

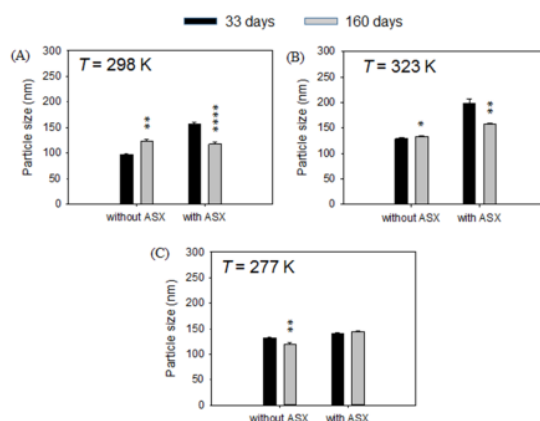
nm, respectively. No significant difference can be observed in the size of the ME with or without ASX. These suggest that both ME@ASX and ME without ASX (Figures 7 and 8) were

**Figure 7.** Stability of T20E-1 at (a) 298, (b) 323, (c) and 277 K during 160 days of storage, all without ASX and loaded with ASX. Asterisks indicate significance analyzed by Tukey's test (*, $P < 0.05$; **, $P < 0.01$; ***, $P < 0.001$; and ****, $P < 0.0001$)

stable. Particle sizes were kept between 96.93 and 204.93 nm at all three different temperatures studied. The thermal stability test suggests that the temperature has an insignificant effect on ME stability.

4. CONCLUSIONS

ME of castor oil, Tween 80, ethanol, and DI water was successfully synthesized. The largest ME area was obtained from a combination of Tween 80 and ethanol with a weight ratio of 2. ME composition of 5 wt.% castor oil, 85 wt.% surfactant mixture, and 10 wt.% water was chosen for further analysis. Astaxanthin as a model lipophilic drug was successfully encapsulated in ME. The ME@ASX showed an

**Figure 8.** Stability of T80E-1 at (a) 298, (b) 323, (c) and 277 K during 160 days of storage, all without ASX and loaded with ASX. Asterisks indicate significance analyzed by Tukey's test (*, $P < 0.05$; **, $P < 0.01$; ***, $P < 0.001$; and ****, $P < 0.0001$)

orange and transparent color with an initial particle size slightly bigger than the parent ME. Within 160 days of storage, both ME and ME@ASX were stable, as indicated by the particle size and polydispersity index value. From the thermal storage test, it shows that the temperature did not influence the stability of the ME. Results of this study suggest the potential of the synthesized ME as a drug carrier matrix. Further studies are needed for ME@ASX in pharmaceutical application, such as the release profile and antimicrobial assay.

■ ASSOCIATED CONTENT

Supporting Information

The Supporting Information is available free of charge at <https://pubs.acs.org/doi/10.1021/acs.jced.0c00341>.

Pseudoternary graph of castor oil with T20 (Acros) as the surfactant and ethanol as the cosurfactant at an S_{mix} of 2, pseudoternary graph of castor oil with T80 as the surfactant and ethanol as the cosurfactant at an S_{mix} of 2 at $T = 310$ K, and the HPLC chromatogram of ME (PDF)

■ AUTHOR INFORMATION

Corresponding Authors

Artik Elisa Angkawijaya – Graduate Institute of Applied Science, National Taiwan University of Science and Technology, Taipei 106, Taiwan; orcid.org/0000-0002-4405-5068; Email: artikelisa@mail.ntust.edu.tw

Suryadi Ismadji – Department of Chemical Engineering, Widya Mandala Surabaya Catholic University, Surabaya 60114, Indonesia; Department of Chemical Engineering, National Taiwan University of Science and Technology, Taipei 106, Taiwan; Email: suryadiismadji@yahoo.com

Authors

Chintya Gunarto – Department of Chemical Engineering, National Taiwan University of Science and Technology, Taipei 106, Taiwan; Department of Chemical Engineering, Widya Mandala Surabaya Catholic University, Surabaya 60114, Indonesia

Yi-Hsu Ju – Graduate Institute of Applied Science, Department of Chemical Engineering and Taiwan Building Technology Center, National Taiwan University of Science and Technology, Taipei 106, Taiwan

Jiayani Nyoo Putro – Department of Chemical Engineering, National Taiwan University of Science and Technology, Taipei 106, Taiwan

Phuong Lan Tran-Nguyen – Department of Mechanical Engineering, Can Tho University, Cantho City 94000, Viet Nam

Felycia Edi Soetaredjo – Department of Chemical Engineering, Widya Mandala Surabaya Catholic University, Surabaya 60114, Indonesia; Department of Chemical Engineering, National Taiwan University of Science and Technology, Taipei 106, Taiwan

Shella Permatasari Santoso – Department of Chemical Engineering, Widya Mandala Surabaya Catholic University, Surabaya 60114, Indonesia; Department of Chemical Engineering, National Taiwan University of Science and Technology, Taipei 106, Taiwan; orcid.org/0000-0003-4698-583X

Aning Ayucitra – Department of Chemical Engineering, National Taiwan University of Science and Technology, Taipei 106, Taiwan; Department of Chemical Engineering, Widya Mandala Surabaya Catholic University, Surabaya 60114, Indonesia

Complete contact information is available at: <https://pubs.acs.org/10.1021/acs.jced.0c00341>

Notes

The authors declare no competing financial interest.

ACKNOWLEDGMENTS

This work was supported partially by Ministry of Science and Technology of Taiwan through the project MOST 108-2221-E-011-106.

REFERENCES

- (1) Zhou, Q.; Xu, J.; Yang, S.; Xue, Y.; Zhang, T.; Wang, J.; Xue, C. The effect of various antioxidants on the degradation of O/W microemulsions containing esterified astaxanthins from *Haematococcus pluvialis*. *J. Oleo Sci.* **2015**, *64*, 515–525.
- (2) Nguyen, V. P.; Kim, S. W.; Kim, H.; Kim, H.; Seok, K. H.; Jung, M. J.; Ahn, Y.-c.; Kang, H. W. Biocompatible astaxanthin as a novel marine-oriented agent for dual chemo-photothermal therapy. *PLoS One* **2017**, *12*, No. e0174687.
- (3) Rostamabadi, H.; Falsafi, S. R.; Jafari, S. M. Nanoencapsulation of carotenoids within lipid-based nanocarriers. *J. Controlled Release* **2019**, *298*, 38–67.
- (4) Tamjidi, F.; Shahedi, M.; Varshosaz, J.; Nasirpour, A. Design and characterization of astaxanthin-loaded nanostructured lipid carriers. *Innovative Food Sci. Emerging Technol.* **2014**, *26*, 366–374.
- (5) Tamjidi, F.; Shahedi, M.; Varshosaz, J.; Nasirpour, A. Stability of astaxanthin-loaded nanostructured lipid carriers in beverage systems. *J. Sci. Food Agric.* **2018**, *98*, 511–518.
- (6) Fassett, R. G.; Coombes, J. S. Astaxanthin: a potential therapeutic agent in cardiovascular disease. *Mar. Drugs* **2011**, *9*, 447–465.
- (7) Odeberg, J. M.; Lignell, A.; Pettersson, A.; Höglund, P. Oral bioavailability of the antioxidant astaxanthin in humans is enhanced by incorporation of lipid based formulations. *Eur. J. Pharm. Sci.* **2003**, *19*, 299–304.
- (8) Ku Aizuddin, K.; Nurlina, M.; Khuriah, A.; Foo, C.; MeorMohd Affandi, M. Development of astaxanthin-loaded biodegradable nanoparticles by nanoprecipitation method. *Int. J. Pharm. Technol.* **2014**, *5*, 5962–5972.
- (9) Hegde, R. R.; Verma, A.; Ghosh, A. Microemulsion: new insights into the ocular drug delivery. *ISRN Pharm.* **2013**, *2013*, 826798.
- (10) Bera, A.; Kumar, T.; Ojha, K.; Mandal, A. Screening of microemulsion properties for application in enhanced oil recovery. *Fuel* **2014**, *121*, 198–207.
- (11) Jha, S. K.; Karki, R.; Venkatesh, D.; Geethalakshami, A. Formulation development & characterization of microemulsion drug delivery systems containing antiulcer drug. *Int. J. Drug Dev. Res.* **2011**, *3*, 336–343.
- (12) Muzaffar, F. A. I. Z. I.; Singh, U. K.; Chauhan, L. Review on microemulsion as futuristic drug delivery. *Int. J. Pharm. Pharm. Sci.* **2013**, *5*, 39–53.
- (13) Thakur, S. S.; Solloway, J.; Stikkelman, A.; Seyfoddin, A.; Rupenthal, I. D. Phase transition of a microemulsion upon addition of cyclodextrin—applications in drug delivery. *Pharm. Dev. Technol.* **2018**, *23*, 167–175.
- (14) Xavier-Junior, F. H.; Vauthier, C.; Morais, A. R. V.; Alencar, E. N.; Egito, E. S. T. Microemulsion systems containing bioactive natural oils: an overview on the state of the art. *Drug Dev. Ind. Pharm.* **2017**, *43*, 700–714.
- (15) Sharma, A. K.; Garg, T.; Goyal, A. K.; Rath, G. Role of microemulsions in advanced drug delivery. *Artif. Cells, Nanomed, Biotechnol.* **2016**, *44*, 1177–1179.
- (16) Attwood, D.; Florence, A. T., Aspects of surfactant toxicity. In *Surfactant Systems: Their chemistry, pharmacy and biology*; Attwood, D., Florence, A. T., Eds.; Springer Netherlands: Dordrecht, 1983; 614–697.
- (17) Food Safety Commission Evaluation Report of Food Additives Polysorbates (Polysorbates 20, 60, 65 and 80). 2007.
- (18) Misik, J.; Vodakova, E.; Pavlikova, R.; Cabal, J.; Novotny, L.; Kuča, K. Acute toxicity of surfactants and detergent-based decontaminants in mice and rats. *Mil. Med. Sci. Lett.* **2012**, *81*, 171–176.
- (19) Abd-Allah, F. I.; Dawaba, H. M.; Ahmed, A. M. Development of a microemulsion-based formulation to improve the availability of poorly water-soluble drug. *Drug Discov Ther* **2010**, *4*, 257–266.
- (20) Badawi, A. A.; Nour, S. A.; Sakran, W. S.; El-Mancy, S. M. S. Preparation and evaluation of microemulsion systems containing salicylic acid. *AAPS PharmSciTech* **2009**, *10*, 1081–1084.
- (21) Calligaris, S.; Valoppi, F.; Barba, L.; Pizzale, L.; Anese, M.; Conte, L.; Nicoli, M. C. Development of transparent curcumin loaded microemulsions by phase inversion temperature (PIT) method: Effect of lipid type and physical state on curcumin stability. *Food Biophys.* **2017**, *12*, 45–51.
- (22) Sha, X.; Wu, J.; Chen, Y.; Fang, X. Self-microemulsifying drug-delivery system for improved oral bioavailability of probucol: preparation and evaluation. *Int. J. Nanomed.* **2012**, *7*, 705.
- (23) Vieira, C.; Evangelista, S.; Cirillo, R.; Lippi, A.; Maggi, C. A.; Manzini, S. Effect of ricinoleic acid in acute and subchronic experimental models of inflammation. *Mediators Inflammation* **2000**, *9*, 223–228.
- (24) Putro, J. N.; Ismadji, S.; Gunarto, C.; Yuliana, M.; Santoso, S. P.; Soetaredjo, F. E.; Ju, Y. H. The effect of surfactants modification on nanocrystalline cellulose for paclitaxel loading and release study. *J. Mol. Liq.* **2019**, *282*, 407–414.
- (25) Eskandani, M.; Hamishehkar, H.; Ezzati Nazhad Dolatabadi, J. Cyto/Genotoxicity study of polyoxyethylene (20) sorbitan mono-laurate (tween 20). *DNA Cell Biol.* **2013**, *32*, 498–503.
- (26) de Oliveira Neves, J. K.; Apolinário, A. C.; Saraiva, K. L. A.; da Silva, D. T. C.; Reis, M. Y. d. F. A.; de Lima Damasceno, B. P. G.; Pessoa, A., Jr.; Galvão, M. A. M.; Soares, L. A. L.; da Veiga Júnior, V. F.; da Silva, J. A.; Converti, A. Microemulsions containing *Copaifera multijuga* Hayne oil-resin: Challenges to achieve an efficient system for β -caryophyllene delivery. *Ind. Crops Prod.* **2018**, *111*, 185–192.
- (27) Munir, R.; Syed, H. K.; Asghar, S.; Khan, I. U.; Rasul, A.; Irfan, M.; Sadique, A. Microemulsion: promising and novel system for drug delivery. *J. Toxicol. Pharmaceut. Sci.* **2017**, *1*, 128–134.

(28) Warisnoicharoen, W.; Lansley, A. B.; Lawrence, M. J. Nonionic oil-in-water microemulsions: the effect of oil type on phase behaviour. *Int. J. Pharm.* **2000**, *198*, 7–27.

(29) Cho, Y.-H.; Kim, S.; Bae, E. K.; Mok, C. K.; Park, J. Formulation of a Cosurfactant-Free O/W Microemulsion Using Nonionic Surfactant Mixtures. *J. Food Sci.* **2008**, *73*, E115–E121.

(30) Basheer, H. S.; Noordin, M. I.; Ghareeb, M. M. Characterization of Microemulsions Prepared using Isopropyl Palmitate with various Surfactants and Cosurfactants. *Trop. J. Pharm. Res.* **2013**, *12*, 305–310.

(31) Delample, M.; Villandier, N.; Douliez, J.-P.; Camy, S.; Condoret, J.-S.; Pouilloux, Y.; Barrault, J.; Jérôme, F. Glycerol as a cheap, safe and sustainable solvent for the catalytic and regioselective β , β -diarylation of acrylates over palladium nanoparticles. *Green Chem.* **2010**, *12*, 804–808.

(32) Li, Y.; Angelova, A.; Liu, J.; Garamus, V. M.; Li, N.; Drechsler, M.; Gong, Y.; Zou, A. *In situ* phase transition of microemulsions for parenteral injection yielding lyotropic liquid crystalline carriers of the antitumor drug bufalin. *Colloids Surf., B* **2019**, *173*, 217–225.

(33) Nazar, M. F.; Khan, A. M.; Shah, S. S. Microemulsion System with Improved Loading of Piroxicam: A Study of Microstructure. *AAPS PharmSciTech* **2009**, *10*, 1286–1294.

(34) Bera, A.; Ojha, K.; Mandal, A.; Kumar, T. Interfacial tension and phase behavior of surfactant-brine–oil system. *Colloids Surf., A* **2011**, *383*, 114–119.

(35) Bera, A.; Mandal, A.; Kumar, T. Physicochemical characterization of anionic and cationic microemulsions: water solubilization, particle size distribution, surface tension, and structural parameters. *J. Chem. Eng. Data* **2014**, *59*, 2490–2498.

(36) Bera, A.; Ojha, K.; Kumar, T.; Mandal, A. Water solubilization capacity, interfacial compositions and thermodynamic parameters of anionic and cationic microemulsions. *Colloids Surf., A* **2012**, *404*, 70–77.

(37) Bera, A.; Ojha, K.; Kumar, T.; Mandal, A. Phase behavior and physicochemical properties of (sodium dodecyl sulfate + brine + propan-1-ol + heptane) microemulsions. *J. Chem. Eng. Data* **2012**, *57*, 1000–1006.

(38) Fink, J. *Chapter 21 - Dispersions, emulsions, and foams*; Gulf Professional Publishing: 2015.

(39) Patravale, V. B.; Date, A. A.; Kulkarni, R. M. Nanosuspensions: a promising drug delivery strategy. *J. Pharm. Pharmacol.* **2004**, *56*, 827–840.

(40) Dehghani, F.; Farhadian, N.; Golmohammadzadeh, S.; Birihae, A.; Ebrahimi, M.; Karimi, M. Preparation, characterization and in-vivo evaluation of microemulsions containing tamoxifen citrate anti-cancer drug. *Eur. J. Pharm. Sci.* **2017**, *96*, 479–489.

(41) Pakkang, N.; Uraki, Y.; Koda, K.; Nithitanakul, M.; Charoensang, A. Preparation of Water-in-Oil Microemulsion from the Mixtures of Castor Oil and Sunflower Oil as Makeup Remover. *J. Surfactants Deterg.* **2018**, *21*, 809–816.

(42) Kumar, A.; Dixit, C. K. 3 - Methods for characterization of nanoparticles. In *Adv. Nanomed. Delivery Ther. Nucleic Acids*; Nimesh, S., Chandra, R., Gupta, N., Eds.; Woodhead Publishing: 2017; 43–58.

(43) Bondi, C. A.; Marks, J. L.; Wroblewski, L. B.; Raatikainen, H. S.; Lenox, S. R.; Gebhardt, K. E. Human and Environmental Toxicity of Sodium Lauryl Sulfate (SLS): Evidence for Safe Use in Household Cleaning Products. *Environ. Health Insights* **2015**, *9*, 27–32.

(44) Kim, Y.-S.; Lee, S.-B.; Lim, C.-H. Effects of Didecyltrimethylammonium Chloride (DDAC) on Sprague-Dawley Rats after 13 Weeks of Inhalation Exposure. *Toxicol. Res.* **2017**, *33*, 7–14.

(45) Barut, K. D.; Ari, F. F. C.; Öner, F. Development and Characterization of a Cationic Emulsion Formulation as a Potential pDNA Carrier System. *Turk. J. Chem.* **2005**, *29*, 27–40.

(46) Patel, S. G.; Rajput, S. J.; Groshev, A.; Sutariya, V. B. Preparation and Characterization of Microemulsion of Cilostazol for Enhancement of Oral Bioavailability. *Curr. Drug Delivery* **2014**, *11*, 531–540.

(47) Li, Y.; Song, J.; Tian, N.; Cai, J.; Huang, M.; Xing, Q.; Wang, Y.; Wu, C.; Hu, H. Improving oral bioavailability of metformin

hydrochloride using water-in-oil microemulsions and analysis of phase behavior after dilution. *Int. J. Pharm.* **2014**, *473*, 316–325.

Effect of a Nonionic Surfactant on the Pseudoternary Phase Diagram and Stability of Microemulsion

ORIGINALITY REPORT

9%

SIMILARITY INDEX

6%

INTERNET SOURCES

8%

PUBLICATIONS

2%

STUDENT PAPERS

PRIMARY SOURCES

- 1** Deski Beri, Septian Budiman, Nofi Yendri Sudiar, Alfajri Yusra, Erianjoni Erianjoni, Ganefri Ganefri, Ali Amran. " Fabrication of ballpoint-ink encapsulating inorganic pigments in microemulsion gels ", RSC Advances, 2022
Publication 2%
- 2** Radu C. Racovita, Maria D. Ciuca, Daniela Catana, Cezar Comanescu, Oana Ciocirlan. "Microemulsions of Nonionic Surfactant with Water and Various Homologous Esters: Preparation, Phase Transitions, Physical Property Measurements, and Application for Extraction of Tricyclic Antidepressant Drugs from Aqueous Media", Nanomaterials, 2023
Publication 1%
- 3** Yaocihuatl Medina-Gonzalez, Séverine Camy, Jean-Stéphane Condoret. " ScCO /Green Solvents: Biphasic Promising Systems for Cleaner Chemicals Manufacturing ", ACS Sustainable Chemistry & Engineering, 2014 1%

4	docksci.com Internet Source	1 %
5	Syntia Lukmanto, Natalia Roesdiyono, Yi-Hsu Ju, Nani Indraswati, Felycia Edi Soetaredjo, Suryadi Ismadji. " SUPERCRITICAL CO EXTRACTION OF PHENOLIC COMPOUNDS IN ROSELLE (L.) ", Chemical Engineering Communications, 2013 Publication	1 %
6	Alchris Woo Go, Ramelito C. Agapay, Yi-Hsu Ju, Angelique T. Conag et al. "The capacity of major countries in Southeast Asia in meeting biodiesel mandates and pursue higher blends based on available major feedstocks", Biofuels, 2020 Publication	1 %
7	Submitted to School of Business and Management ITB Student Paper	1 %
8	www.semanticscholar.org Internet Source	1 %
9	link.springer.com Internet Source	1 %
10	Faranak Dehghani, Nafiseh Farhadian, Shiva Golmohammadzadeh, Amir Birihaee, Mahmoud Ebrahimi, Mohammad Karimi.	1 %

"Preparation, characterization and in-vivo evaluation of microemulsions containing tamoxifen citrate anti-cancer drug", European Journal of Pharmaceutical Sciences, 2017

Publication

11

Elda Melwita, Yeshitila Asteraye Tsigie, Suryadi Ismadji, Yi-Hsu Ju. "PURIFICATION OF AZADIRACHTIN VIA SILICA GEL COLUMN CHROMATOGRAPHY", Journal of Liquid Chromatography & Related Technologies, 2011

Publication

1 %

Exclude quotes On

Exclude matches < 1%

Exclude bibliography On